

# Fabrication of silicon microwire arrays for photovoltaic applications

Ning Guo · Jinquan Wei · Qinke Shu · Yi Jia · Zhen Li ·  
Kun Zhang · Hongwei Zhu · Kunlin Wang ·  
Shuang Song · Ying Xu · Dehai Wu

Received: 24 February 2010 / Accepted: 22 July 2010 / Published online: 31 August 2010  
© Springer-Verlag 2010

**Abstract** A novel method of combining photolithography, wet chemical etching and oxidation process was proposed to fabricate large area of silicon microwire (SiMW) arrays. The dimensions of the SiMWs can be easily controlled by photomask and etching conditions. Solar cells based on the heterojunction between SiMW and double-walled carbon nanotubes (DWNTs) were constructed. The initial test on the DWNT/SiMW shows efficiency ( $\eta$ ) of 0.59%. By adding a few drops of HBr/B<sub>2</sub> electrolyte, the efficiency was improved to 1.96% with  $J_{sc} = 19.2 \text{ mA/cm}^2$  and  $V_{oc} = 0.35 \text{ V}$ , FF = 29.2%, showing the potential of SiMWs in photovoltaic applications.

## 1 Introduction

Silicon is the first of photovoltaic materials used in solar cells. Si-based solar cells, with moderate efficiency and relative high price, still dominate the current photovoltaic market. In order to improve the efficiency and reduce the overall cost, new materials and novel technology, especially nanomaterials and nanotechnology, were introduced to the

Si-based solar cells [1–5]. However, there are some gaps in efficiency between these new devices and the commercial monocrystalline planar Si solar cells. Recently, we constructed a carbon-nanotube-on-Si (CNT/Si) heterojunction solar cell model [6, 7], and up to now, gained the best conversion efficiency ( $\eta$ ) of 7.4% [7]. A hybrid solar cell, consisted of a heterojunction cell and a photoelectrochemical (PEC) cell among CNTs, Si nanowires (SiNWs) and HBr/Br<sub>2</sub> redox electrolyte, was also proposed [8]. Although the present efficiency of the heterojunction (or hybrid) cell is not so high, it is still a promising solar cell. One way might lead to higher efficiency for the CNT/Si heterojunction solar cell is to provide more effective interface to capture more solar energy and generate more excitons. But larger interface also means higher possibility of recombination for the excitons. By comprehensively considering the interface and recombination, Si microwire (SiMW) arrays might be a good architecture for high efficiency of the CNT/Si heterojunction solar cell. Furthermore, it has been reported that diffusion length of photogenerated carriers in Si nanowires (SiNWs) reaches about 2  $\mu\text{m}$  [9], which indicates that Si wires with a few microns in size are sufficient to get high efficiency.

Inductively coupled plasma (ICP) etching method is generally used to fabricate Si microstructure [10]. But this method has not been widely used in photovoltaic devices due to its low fabricating efficiency and high cost. Recently, several methods were reported to fabricate nano- or micro- Si wires [11–17], including deep reactive ion etching [11, 12], wet chemical etching [13–15], and chemical vapor deposition [16, 17]. Among these methods, wet chemical etching might be the most promising method to fabricate nano- and/or microwires in large area due to its low cost and easy to be industrialized. Here, we report a novel method to fabricate SiMW arrays in large area by combining the photolithography, wet chemical etching and oxida-

**Electronic supplementary material** The online version of this article (doi:10.1007/s00339-010-6009-1) contains supplementary material, which is available to authorized users.

N. Guo · J. Wei (✉) · Q. Shu · Y. Jia · Z. Li · K. Zhang · H. Zhu ·  
K. Wang · D. Wu

Key Lab for Advanced Materials Processing Technology  
of Education Ministry, Department of Mechanical Engineering,  
Tsinghua University, Beijing 100084, China  
e-mail: jqwei@tsinghua.edu.cn  
Fax: +86-10-62770109

S. Song · Y. Xu  
Beijing Solar Energy Research Institute, Beijing 100083, China

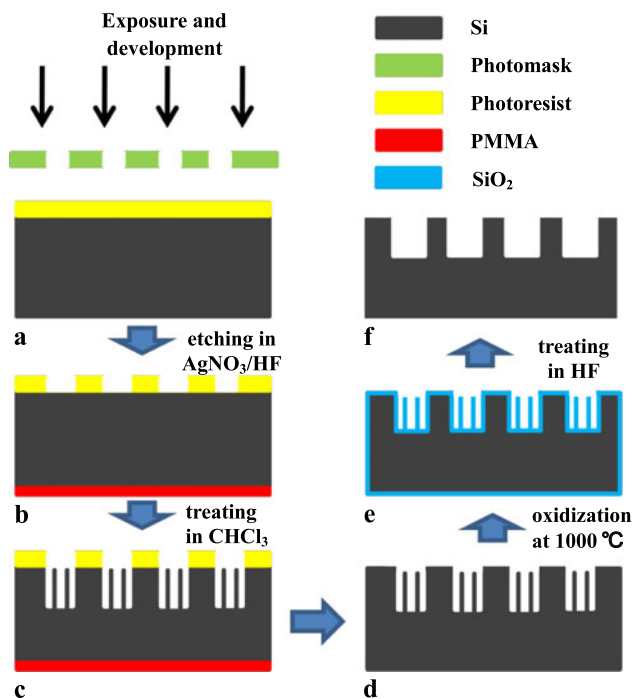


**Fig. 1** Schematic illustration of steps for fabricating Si microwire array from Si wafer

tion process, which can tailor the dimensions of the SiMW arrays easily. We also explore the photovoltaic properties of DWNT/SiMW heterojunction solar cells with and without HBr/Br<sub>2</sub> electrolyte, respectively.

## 2 Experiment

Figure 1 shows a schematic illustration of the SiMW array fabrication process. Firstly, a layer ( $\sim 1 \mu\text{m}$ ) of positive photoresist (Fuji 6400 L) was spin coating onto a n-type (100) Si wafer (4 inch,  $400 \pm 10 \mu\text{m}$  thick,  $2\text{--}4 \Omega\text{cm}$ ). The photoresist was then exposed to ultraviolet light through a photomask with predefined patterns (Fig. 1a). After removing the unexposed photoresist in developer solution, Si wafer with desired patterns of photoresist was obtained. Secondly, to protect the other side of the wafer, the Si wafer was covered by a layer of polymethylmethacrylate (PMMA) at the backside by spin coating (Fig. 1b). Thirdly, the wafer was then etched in solution of AgNO<sub>3</sub>/HF (0.02 M/5 M) at 50°C for 2 to 10 min according to the desired height of microwires. When the Ag dendrites, forming during the etching process, were removed in HNO<sub>3</sub> solution, a mixed structure of SiMW and SiNW arrays was obtained (Fig. 1c). Fourthly, the photoresist patterns and PMMA were removed in trichloromethane (CHCl<sub>3</sub>) solution (Fig. 1d). Fifthly, in order to get rid of the SiNWs, the Si wafer was oxidized in an atmosphere of nitrogen and water vapor (N<sub>2</sub>/H<sub>2</sub>O = 10:1, atomic ratio) at 1000°C for two hours (Fig. 1e). Finally, the

oxidized silicon was immersed in HF (10 vol.%) and then rinsed in deionized water to totally remove SiNWs (Fig. 1f).

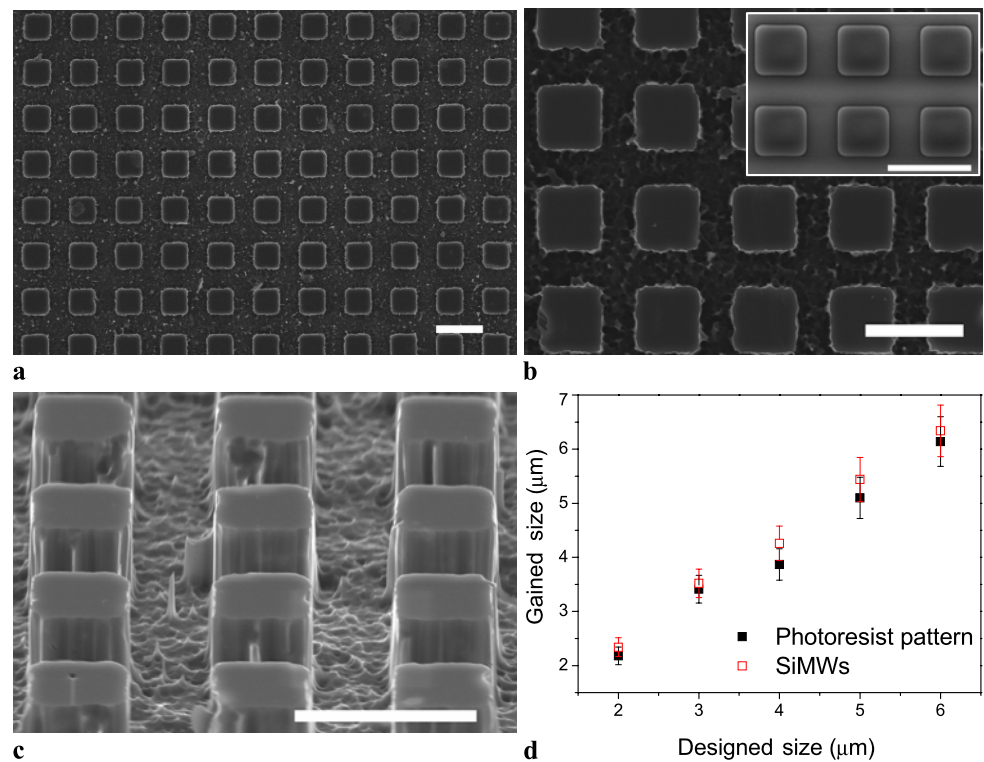
Macroscopic double-walled carbon-nanotube (DWNT) films were prepared by the CVD method and then purified in H<sub>2</sub>O<sub>2</sub> and HCl solution [18, 19]. DWNT/SiMW heterojunction solar cells were fabricated by the method reported recently [7]. In brief, the SiMW arrays were cut into small pieces with dimension of  $1 \times 1 \text{ cm}^2$ . A Ti/Pd/Ag layer, acting as the back electrode, was sputtered to the back side of the silicon substrate. A black insulating tape ( $1 \times 1 \text{ cm}^2$ ) with a round window (6 mm in diameter) covered on the top of the SiMW arrays. A purified DWNT film was then directly transferred to the SiMW array. Annealed copper wires were connected to the front (DWNT film) and back (Ti/Pd/Ag) electrodes using silver paint. The DWNT/SiMW solar cells were tested using a solar simulator (Thermo Oriel 91192-1000) under AM 1.5G ( $100 \text{ mW}/\text{cm}^2$ ). The DWNT film was connected as anode, and Ti/Pd/Ag as cathodes.

## 3 Results and discussion

The SiMW arrays were examined by scanning electron microscope (SEM, LEO 1530). By designing the photomask, large area of the SiMW arrays with desired shapes and size can be easily obtained. For example, we designed square pattern arrays with different sizes (2  $\mu\text{m}$ , 3  $\mu\text{m}$ , 4  $\mu\text{m}$ , 5  $\mu\text{m}$ , and 6  $\mu\text{m}$ , respectively) and a fixed center distance of 10  $\mu\text{m}$ . Figure 2a presents a SEM image of a large area of and highly reduplicate SiMW array with square shape ( $5.0 \times 5.0 \mu\text{m}$ ). Due to the vertical etching of Si in AgNO<sub>3</sub>/HF solution, the SiMWs stand vertically to the Si wafer. We examined and evaluated the size precision of the obtained SiMWs by SEM. Figure 2b presents a SEM image of the SiMWs obtained by using a photomask with designed patterns of  $6.0 \times 6.0 \mu\text{m}$ . The size of the SiMW is about  $6.4 \times 6.4 \mu\text{m}$ , which is slightly larger than that of the photoresist pattern ( $6.2 \times 6.2 \mu\text{m}$ , inset in Fig. 2b), and also larger than that of the designed pattern. The size difference among the designed photomask, photoresist patterns and obtained SiMWs is given in Fig. 2d. It shows that the size of the obtained SiMWs are slightly larger ( $\sim 5\text{--}10\%$ ) than those of photoresist patterns. To get Si wires with more accurate size, it needs to optimize the oxidation parameters in the N<sub>2</sub>/H<sub>2</sub>O ambient.

When the SiO<sub>2</sub> layer ( $\sim 100 \text{ nm}$  in thickness) removed by HF solution is taken into account, the size of SiMWs obtained after etching in AgNO<sub>3</sub>/HF solution are larger than those of the photoresist patterns. It means that the etching of SiMW in AgNO<sub>3</sub>/HF solution begins at about 200–300 nm away from the edge of the photoresist patterns. The shapes of the SiMW inherit those of the photoresist patterns quite well. The top surfaces of the SiMWs are very smooth, which

**Fig. 2** SEM images of the SiMW arrays. **(a)** Large area SiMW array with dimensions of  $5 \times 5 \times 5 \mu\text{m}$ . **(b)** SiMW array with designed size of  $6 \times 6 \mu\text{m}$ . *Inset:* the photoresist pattern. **(c)** Tilted-view (ca.  $30^\circ$ ) image of the SiMW arrays with dimensions of  $4 \times 4 \times 5 \mu\text{m}$ . **(d)** The accuracy of the processing. Scale bar:  $10 \mu\text{m}$



indicates that photoresist can protect the Si from etching during the etching process. But the sidewalls of the SiMWs are not as smooth as those fabricated by ICP or CVD methods [10, 17]. There are some small trenches on the SiMW, which might result from etching by the Ag dendrites during the etching process. The bottoms of the SiMW array are rough after removing the SiNWs in HF solution.

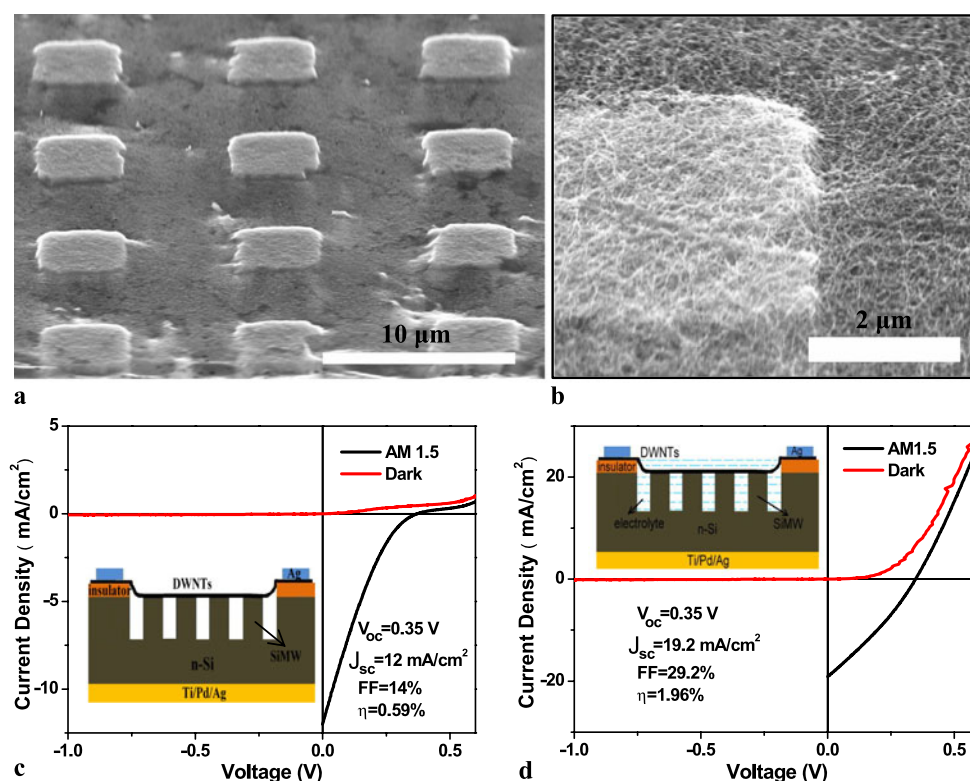
The height of the SiMW arrays can be easily controlled by the etching time in  $\text{AgNO}_3/\text{HF}$  solution. Figure 2c shows a SiMW array with a height of  $6 \mu\text{m}$  after 15 min etching. The etching rate of SiMW is about  $0.4 \mu\text{m}/\text{min}$ , which is similar to that reported in the literature [13]. Due to insufficient oxidation in hot  $\text{N}_2/\text{H}_2\text{O}$  ambient, some residual SiNWs in the trenches of SiMW arrays are still identified in Fig. 2c. By extending the oxidation time, the residual nanowires can be totally removed and the sidewalls of the SiMWs become smoother. It is easy to fabricate large area of (e.g. 4 inch in diameter) SiMW arrays with desired dimensions and shapes by this method.

Our recent work shows that DWNTs and planar Si wafer (n-type) can construct heterojunction solar cell, which convert solar energy into electricity [6, 7]. The performance of the DWNT/Si heterojunction solar cell, especially short current density ( $J_{\text{sc}}$ ) and efficiency ( $\eta$ ), were influenced by the interface of heterojunction. The SiMW array can provide more active surface for the heterojunction than the planar Si wafer, which is expected to have higher efficiency if all the SiMW surfaces are covered by DWNTs. We fabricated

a DWNT/SiMW heterojunction solar cell using the same method [6, 7] only replacing planar Si with SiMW array.

Figure 3a shows a tilted-view (ca.  $60^\circ$ ) SEM image of the DWNT film depositing on a SiMW array with dimensions of  $4 \times 4 \times 5 \mu\text{m}$ . It shows that DWNT film does not cover all the surface of the SiMWs. It covers only the tip of SiMW arrays. A high magnification SEM image in Fig. 3b shows that DWNTs film contact with the SiMW tips quite well. Figure 3c is a dark  $J-V$  curve of the DWNT/SiMW heterojunction, which shows a rectification effect of the heterojunction. Due to the relative high contact resistance ( $\sim 500 \Omega$ ), the observed rectification is quite minimal. When the DWNT/SiMW solar cell is exposed under a solar simulator at AM 1.5G ( $100 \text{ mW}/\text{cm}^2$ ), it shows an evident photovoltaic effect with an open-circuit voltage ( $V_{\text{oc}}$ ) of  $0.35 \text{ V}$ , short-circuit current density ( $J_{\text{sc}}$ ) of  $12 \text{ mA}/\text{cm}^2$ , filled factor (FF) of 14%, and conversion efficiency ( $\eta$ ) of 0.59%, respectively (see Fig. 3c). The efficiency of the DWNT/SiMW solar cell is lower than that of our previous DWNT/Si (n-type planar Si) solar cells [7]. The relative low efficiency of the DWNT/SiMW cell might result from two reasons: reduction in heterojunction interface and increase of surface defects. In Fig. 3a, DWNTs cover only the top of the SiMWs (about  $200 \text{ nm}$  in depth). As shown in inset of Fig. 3c, the heterojunction forms only on the tips of the SiMW, which means that interface of the DWNT/SiMW heterojunction occupies only 20% of the total Si surface. A higher efficiency is expected for the DWNT/SiMW heterojunction solar cell if all the SiMW surfaces are covered

**Fig. 3** (a) A SEM image of the DWNT/SiMW heterojunction solar cell. (b) High magnification SEM image. (c) Dark and bright  $J$ - $V$  curves of the DWNT/SiMW heterojunction solar cell. Inset: schematic image of the DWNT/SiMW heterojunction cell. (d) Dark and bright  $J$ - $V$  curves of the DWNT/SiMW hybrid solar cell with HBr/Br<sub>2</sub> electrolyte. Inset: schematic image of the DWNT/SiMW hybrid solar cell



by DWNTs. At the same time, the sidewalls and bottom of the SiMW arrays are rough, which increase the possibility of recombination for the exciton. To improve the efficiency of the DWNT/SiMW heterojunction solar cells, it needs to fabricate SiMW with smooth surface and low surface defects.

A band diagram of the DWNT/SiMW heterojunction is given in Fig. 4a. We estimate the band gap the semiconductive DWNTs ( $d = 1.5$ – $3$  nm) used in the experiments are less than  $0.5$  eV according to  $E_g = 0.798/d$  [20]. The work function of the DWNTs is around  $4.8$  eV [21]. For the n-type SiMW arrays, the band gap and conduction level (relative to vacuum level) are about  $1.12$  eV and  $-4.05$  eV, respectively; while the Fermi level is  $-4.31$  eV, about  $0.26$  eV below the conduction band, for a dopant concentration of  $1 \times 10^{15}$  cm<sup>-3</sup> [22]. When the DWNT/SiMW heterojunction solar cell is illustrated by light, it forms a built-in voltage of  $0.49$  eV according to the band diagram in Fig. 3a. The  $V_{oc}$  of the heterojunction is lower than the built-in voltage, indicating a high series resistance in the solar cell. Charge separation occurs at this built-in field, where electrons are directed to the SiMW arrays and holes are transported through the DWNTs.

We add a few drops of electrolyte, composed of 40% hydrobromic acid and 3% bromine (HBr/Br<sub>2</sub>), to the same device tested above to form a hybrid solar cell [8]. The structure of the hybrid solar cell is given in inset of Fig. 3d. The Dark  $J$ - $V$  curve of the hybrid solar cell is shown in Fig. 3d. The hybrid solar cell behaves better rectification effect than

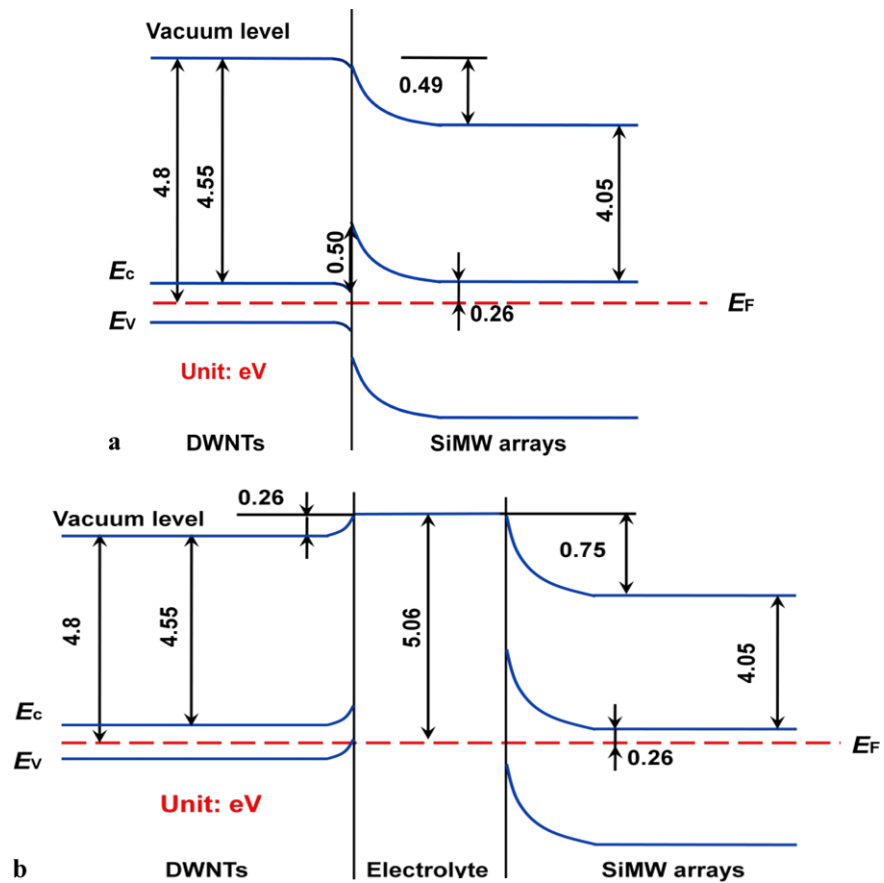
the DWNT/SiMW cell. The electrolyte can improve the interface of DWNT/SiMW heterojunction by providing effective transport channels for charge carriers, which reduces the series resistance of the device.

A band diagram of the hybrid solar cell is shown in Fig. 4b. The equilibrium electrode potential of HBr/Br<sub>2</sub> is tested to be  $0.56$  eV (relative to standard hydrogen electrode), so the Fermi level is  $-5.06$  eV. The built-in voltage at the interface of SiMW arrays and electrolyte is  $0.75$  eV, driving the electrons into the SiMW arrays and holes into the electrolyte. The electrolyte of HBr/Br<sub>2</sub> can not only establish a redox reaction on the surface of DWNTs and SiMWs, but also transport the photogeneration carriers from SiMW to DWNT film.

Figure 3d shows a bright  $J$ - $V$  curve of the hybrid solar cell illuminated under the solar simulator (AM 1.5G). It shows a performance of  $V_{oc} = 0.35$  V,  $J_{sc} = 19.2$  mA/cm<sup>2</sup>, FF = 29.2%, and  $\eta = 1.96\%$ . The efficiency of DWNT/SiMW with HBr/Br<sub>2</sub> electrolyte is about 2 times higher than that without electrolyte. The enhancement in efficiency comes mainly from the increase of  $J_{sc}$  as well as the decrease of the series resistance. Although optical reflection of the SiMW array is higher than that of the SiNW array (see Fig. 1S), the efficiency of the hybrid cell is improved  $\sim 50\%$  by simply replace the SiNW with SiMW arrays [8]. The increase of efficiency might result from more effective interface of SiMWs with the DWNTs than the SiNWs. The surface of the SiNWs is larger than that of the SiMWs. But



**Fig. 4** Band diagrams of DWNT/SiMW photovoltaic device with and without HBr/Br<sub>2</sub> electrolyte. (a) DWNT/SiMW heterojunction solar cell without electrolyte. (b) DWNT/SiMW hybrid solar cell with electrolyte



most of the SiNW surfaces are not contact with DWNTs to form heterojunction. As one knows, the increase of surface area will increase the short-circuit current. But the large surface area will also increase possibility of surface recombination for exciton. In our case, the higher efficiency of hybrid cell with SiMWs than with SiNWs might contribute to the increase the interface of heterojunction and also to the decrease of surface recombination of excitons. So it might be an effective way to further improve the short-circuit current and conversion efficiency by fabricating Si wires with smooth sidewalls and bottom to reduce the surface recombination of excitons.

#### 4 Conclusions

In summary, well-aligned SiMW arrays with controllable sizes have been fabricated by combining the photolithography, wet chemical etching and oxidation process. It is a convenient method to fabricate Si microstructure in large area. The dimensions of the Si wires can be determined by designing the photomask and etching conditions. A hybrid solar cell basing on the SiMW arrays, DWNTs and electrolyte was fabricated. A conversion efficiency of 1.96% is obtained, which is higher than our previous similar device

made of SiNW arrays. The SiMW arrays show potential in photovoltaic applications.

**Acknowledgements** This work is financially supported by 863 Program (Grant No. 2009AA05Z423), Foundation for the Author of National Excellent Doctoral Dissertation (Grant No. 2007B37) Key Project of Ministry of Education (Grant No. 108006), China.

#### References

1. B.Z. Tian, X.L. Zheng, T.J. Kempa, Y. Fang, N.F. Yu, G.H. Yu, J.L. Huang, C.M. Lieber, *Nature* **449**, 885 (2007)
2. H. Fang, X.D. Li, S. Song, Y. Xu, J. Zhu, *Nanotechnology* **19**, 255703 (2008)
3. V. Sivakov, G. Andrae, A. Gawlik, A. Berger, J. Plentz, F. Falk, S.H. Christiansen, *Nano Lett.* **9**, 1549 (2009)
4. J. Yoon, A.J. Baca, S.I. Park, P. Elvikis, J.B. Geddes, L.F. Li, R.H. Kim, J.L. Xiao, S.D. Wang, T.H. Kim, M.J. Motala, B.Y. Ahn, E.B. Duoss, J.A. Lewis, R.G. Nuzzo, P.M. Ferreira, Y.G. Huang, A. Rockett, J.A. Rogers, *Nature Mater.* **7**, 907 (2008)
5. K.E. Plass, M.A. Filler, J.M. Spurgeon, B.M. Kayes, S. Maldonado, B.S. Brunschwig, H.A. Atwater, N.S. Lewis, *Adv. Mater.* **21**, 325 (2009)
6. J.Q. Wei, Y. Jia, Q.K. Shu, Z.Y. Gu, K.L. Wang, D.M. Zhuang, G. Zhang, Z.C. Wang, J.B. Luo, A.Y. Cao, D.H. Wu, *Nano Lett.* **7**, 2317 (2007)
7. Y. Jia, J.Q. Wei, K.L. Wang, A.Y. Cao, Q.K. Shu, X.C. Gui, Y.Q. Zhu, D.M. Zhuang, G. Zhang, B.B. Ma, L.D. Wang, W.J. Liu, Z.C. Wang, J.B. Luo, D.H. Wu, *Adv. Mater.* **20**, 4594 (2008)

8. Q.K. Shu, J.Q. Wei, K.L. Wang, H.W. Zhu, Z. Li, Y. Jia, X.C. Gui, N. Guo, X.M. Li, C.R. Ma, D.H. Wu, *Nano Lett.* **9**, 4338 (2009)
9. M.D. Kelzenberg, D.B. Turner-Evans, B.M. Kayes, M.A. Filler, M.C. Putnam, N.S. Lewis, H.A. Atwater, *Nano Lett.* **8**, 710 (2008)
10. U. Sokmen, A. Stranz, S. Fundling, H.H. Wehmann, V. Bandalo, A. Bora, M. Tornow, A. Waag, E. Peiner, J. *Micromech. Microeng.* **9**, 105005 (2009)
11. K.J. Morton, G. Nieberg, S.F. Bai, S.Y. Chou, *Nanotechnology* **19**, 345301 (2008)
12. J. Baca, M.A. Meitl, H.C. Ko, S. Mack, H.S. Kim, J.Y. Dong, P.M. Ferreira, J.A. Rogers, *Adv. Funct. Mater.* **17**, 3051 (2007)
13. K.Q. Peng, Z.P. Huang, J. Zhu, *Adv. Mater.* **16**, 73 (2004)
14. Z.P. Huang, H. Fang, J. Zhu, *Adv. Mater.* **19**, 744 (2007)
15. K.Q. Peng, X. Wang, X.L. Wu, S.T. Lee, *Appl. Phys. Lett.* **95**, 143119 (2009)
16. J.D. Holmes, K.P. Johnston, R.C. Doty, B.A. Korgel, *Science* **287**, 1471 (2000)
17. J.M. Spurgeon, K.E. Plass, B.M. Kayes, B.S. Brunschwig, H.A. Atwater, N.S. Lewis, *Appl. Phys. Lett.* **93**, 032112 (2008)
18. J.Q. Wei, L.J. Ci, B. Jiang, Y.H. Li, X.F. Zhang, H.W. Zhu, C.L. Xu, D.H. Wu, *J. Mater. Chem.* **13**, 1340 (2003)
19. J.Q. Wei, H.W. Zhu, Y.H. Li, B. Chen, Y. Jia, K.L. Wang, Z.C. Wang, W.J. Liu, J.B. Luo, M.X. Zheng, D.H. Wu, Y.Q. Zhu, B.Q. Wei, *Adv. Mater.* **18**, 1695 (2006)
20. J.W. Mintmire, C.T. White, *Carbon* **33**, 893 (1995)
21. P. Liu, Q. Sun, F. Zhu, K. Liu, K.L. Jiang, L. Liu, Q.Q. Li, S.S. Fan, *Nano Lett.* **8**, 647 (2008)
22. S.M. Sze, *Physics of Semiconductor Devices*, 2nd edn. (Wiley, New York, 1981)